Superelastic scattering of electrons from metastable He-like C^{4+} and O^{6+} ions

A. S. Alnaser,[1] A. L. Landers,[1] D. J. Pole,[1] S. Hossain,[1] O. A. Haija,[1] T. W. Gorczyca,[1] J. A. Tanis,[1] and H. Knutson[1,2]
[1]*Department of Physics, Western Michigan University, Kalamazoo, Michigan 49008*
[2]*Johns Hopkins University, Baltimore, Maryland 21218*
(Received 20 November 2001; published 21 March 2002)

Superelastic scattering, a collision process in which the scattered electron gains energy, has been investigated for metastable $C^{4+}(1s2s\,^3S)$ and $O^{6+}(1s2s\,^3S)$ He-like ions colliding with quasifree H_2-target electrons. The measured superelastic-scattering cross sections for $1s2s\,^3S \rightarrow 1s^2\,^1S$ deexcitation show a strong dependence on the collision energy and the atomic number of the He-like ion. *R*-matrix calculations for the time-reversed equivalent process of electron-impact excitation are compared with the measured cross sections through the principle of detailed balance. In these calculations, the impulse approximation is utilized in conjunction with the Compton profile of the target electrons for the collisions of ions with quasifree electrons studied here. Calculations were performed taking into account the anisotropy of the cross sections as a function of the scattering angle, which equals 180° in the projectile rest frame for the reported measurements. Comparison between theory and experiment was used to infer the metastable $1s2s\,^3S$ fraction in the incident He-like beam.

DOI: 10.1103/PhysRevA.65.042709 PACS number(s): 34.50.Fa, 34.80.Dp, 34.80.Kw

I. INTRODUCTION

Electron collisions with multiply charged ions are of fundamental interest and are important for the understanding of laboratory and astrophysical plasmas. Common processes occurring in such collisions are the elastic and inelastic scattering of electrons. In these collisions, the scattered electron either preserves its energy (elastic) or transfers some of its energy to the ion and excites it from the ground state to an excited state (inelastic).

In addition to elastic and inelastic scattering, an electron may interact with an ion in an initially excited metastable state, for example, $1s2s\,^3S$, with the result that the electron deexcites the ion, thereby gaining an amount of energy equal to the excitation energy of the metastable state above the ground state. In such an event the electron is said to be *superelastically* scattered. Thus, superelastically scattered electrons have energies higher than elastically scattered ones. The superelastic reaction of interest here can be written as

$$e^-(E_i) + A^{q+}(1s2s\,^3S) \rightarrow A^{q+}(1s^2\,^1S) + e^-(E_f), \tag{1.1}$$

where $q = Z - 2$ is the ionic charge, E_i is the energy of the incoming electron, $E_f = E_i + \Delta E$ is the final energy of the electron, and ΔE is the $1s^2\,^1S \rightarrow 1s2s\,^3S$ transition energy. A schematic energy diagram for the superelastic-scattering process is shown in Fig. 1. Superelastic scattering of electrons can be viewed as the time-reversed process of inelastic scattering, i.e., electron-impact excitation.

The deexcitation of metastable excited states following collisions with electrons can be investigated by detecting the energies of the outgoing electrons. The investigation of superelastic scattering of electrons has been an important tool in studying the alignment and orientation of excited-state metastable atoms by providing valuable information about different scattering parameters [1–3]. Different techniques have been employed in the investigation of superelastic scattering of electrons. Williams *et al.* [4] have reported measurements for superelastically scattered electrons gaining an energy of ~4.5 eV in the deexcitation of C^+ from the metastable $1s^22s2p^2\,^4P$ state to the $1s^22s^22p\,^2P$ ground state. The C^+ beam was extracted from a Penning-type discharge source, which usually provides a sufficient fraction of metastable states. Jacka *et al.* [5] have measured superelastically scattered electrons that gained an energy of ~20 eV from laser-excited metastable $1s2p\,^3P_2$ helium atoms deexcited to the ground state $1s^2\,^1S_0$. For the time-reversed equivalent process of electron-impact excitation, Bannister *et al.* [6] used a merged electron-ion-beam energy-loss method to measure resonance structure in the total cross section for near-threshold electron-impact excitation of the $4s^2\,^1S \rightarrow 4s4p\,^3P$ intercombination transition in Kr^{6+}. Similar techniques were used to study the superelastic scattering of electrons from other metastable targets [7,8]. Very recently, using 0°-projectile electron spectroscopy, Závodosky *et al.* [9] reported measurements for superelastically scattered electrons in collisions between metastable $F^{7+}(1s2s\,^3S)$ ions and quasifree electrons from an H_2 target. The fluorine beam was obtained from a tandem Van de Graaff accelerator. Subsequent stripping of such beams usually results in a significant fraction of metastable ions [10].

In the case of ions interacting with light targets (H_2, for example), the target electrons are loosely bound or *quasifree*. Thus, the target electrons have an average collision velocity equal to the projectile velocity in the projectile frame of ref-

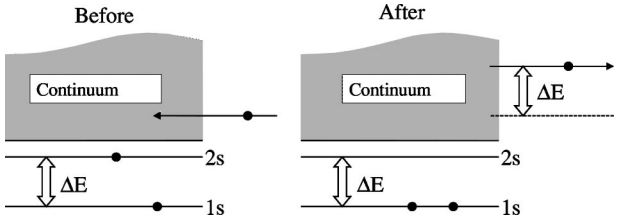

FIG. 1. Schematic energy diagram for superelastic scattering. An incident electron deexcites a 2*s* electron to 1*s*, gaining an energy ΔE [see Eq. (1.1)].

erence. The energy distribution of these electrons is determined by its corresponding Compton profile in the target atom or molecule. For intermediate to high-velocity collisions, where the projectile velocity is much larger than the orbital velocity of the target electron, the *impulse approximation* is valid [11,12]. Using this approximation, in conjunction with the Compton profile of the active electron [13], elastic [14–16] and inelastic [17–19] scattering of quasifree electrons from heavy ions have been investigated and well understood. Thus, this approximation can also be used to obtain the cross sections for superelastic scattering from a metastable state to the ground state, which is just the time-reversed process of inelastic scattering from the ground state to the metastable state.

In the present work, a detailed experimental and theoretical investigation of the superelastic scattering of quasifree H_2 target electrons from metastable $C^{4+}(1s2s\,^3S)$ and $O^{6+}(1s2s\,^3S)$ ions is reported. These results, combined with earlier ones for $F^{7+}(1s2s\,^3S)$ [9], allow us to explore the effect of the atomic number of the He-like ion on the superelastic scattering cross section. Different collision velocities were used in the case of C^{4+} metastable ions, providing insight into the strong dependence of the superelastic cross section on the collision velocity. By comparing the present experimental results with theoretical ones, the metastable $1s2s\,^3S$ fraction of the He-like ions in the incident beam can be inferred for each collision velocity.

II. EXPERIMENTAL PROCEDURE

The experiment was performed at Western Michigan University using the tandem Van de Graaff accelerator. Oxygen and carbon ions were accelerated to the desired energies, and then the beams were poststripped to obtain He-like C^{4+} and O^{6+} ions. Such He-like beams usually contain a significant fraction of metastable $1s2s\,^3S$ ions [10], which is essential for investigating the superelastic-scattering process. After selection by an analyzing magnet, the beam was collimated and directed into the collision chamber. The chamber was located at a distance of about 3 m from the stripping foils, such that more than 99% of the long-lived metastable $1s2s\,^3S$ ions produced in the foils do not decay before reaching the target. The lifetimes of this state in C^{4+} and O^{6+} are 0.02 sec and 960 μsec, respectively [20]. Following collisions with the H_2 target, the projectile ions were collected in a Faraday cup for normalization. Care was taken to maintain single-collision conditions by making measurements for several gas pressures. Gas pressures for the measurements were always less than 40 mTorr.

A tandem 45° parallel-plate electron spectrometer with a channeltron detector, as shown in Fig. 2, was positioned at 0° relative to the incident beam and used to analyze the energy of the outgoing electrons following the collisions. The spectrometer had an energy resolution of ~3%. Electron counts from the channeltron detector were normalized to the incident-beam intensity as measured by the suppressed Faraday cup. The absolute efficiency of the spectrometer was determined by comparing the measured intensity for elastically scattered (binary-encounter) electrons with the calculated cross sections obtained using the impulse approximation, as done in previous works [9,14,19]. The efficiency of the spectrometer was then used to convert the measured electron yields to absolute differential cross sections. The beam-induced electron background was determined by taking spectra without gas in the target cell. The resulting electron yield was found to be negligible as a source of error.

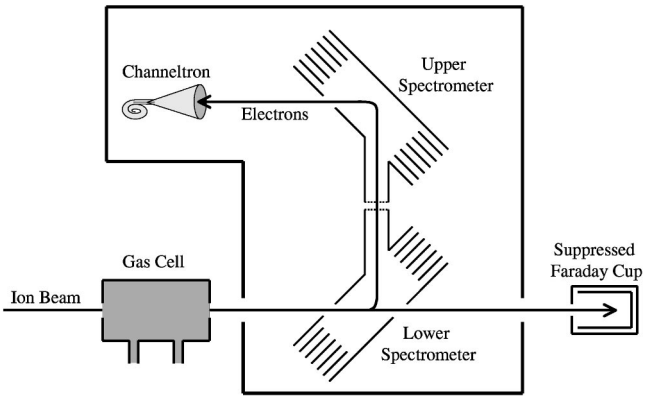

FIG. 2. Schematic of the 0° tandem parallel-plate electron spectrometer used to analyze the energies of the outgoing electrons. The energy resolution of the spectrometer is ~3%.

III. THEORETICAL ANALYSIS

As noted above, superelastic scattering is just the time-reversed process of inelastic electron scattering. Then, from the principle of detailed balance

$$\frac{d\sigma_{i\to f}}{d\Omega}^{superelastic} = \frac{\omega_f k_f^2}{\omega_i k_i^2}\frac{d\sigma_{f\to i}}{d\Omega}^{excitation}, \qquad (3.1)$$

where ω_i and ω_f are the statistical weights of the initial and final states, respectively, and k_i^2 and k_f^2 are the initial and final energies of the electron, respectively. In the present case of superelastic scattering from an initial S state ($L_i=0$) to a final S state ($L_f=0$), the initial and final angular momenta for a given partial wave are equal ($l_i=l_f\equiv l$), so that the expression for angular differential cross section [21] is simplified considerably, and is given in atomic units by

$$\begin{aligned}\frac{d\sigma_{if}}{d\Omega} &= \frac{1}{8k_i^2}\sum_{\lambda}(2\lambda+1)P_\lambda(\cos\theta)\\ &\times\sum_{l,l'}2(2l+1)(2l'+1)\begin{pmatrix} l & l' & \lambda\\ 0 & 0 & 0\end{pmatrix}^2\\ &\times\exp\{[\sigma_l(E_i)+\sigma_l(E_f)-\sigma_{l'}(E_i)-\sigma_{l'}(E_f)]\}\\ &\times T^*_{l'l'}(i\to f)T_{ll}(i\to f), \qquad (3.2)\end{aligned}$$

where k_i^2 is the energy of the incoming electron, l and l' are the orbital angular momenta of the scattered electron, $\sigma_l=\arg[\Gamma(l+1+iq/k)]$ is the Coulomb phase shift, and $T_{ll}(i\to f)$ is the transition-matrix element from state i to state f. The sums are performed over the multipole-expansion pa-

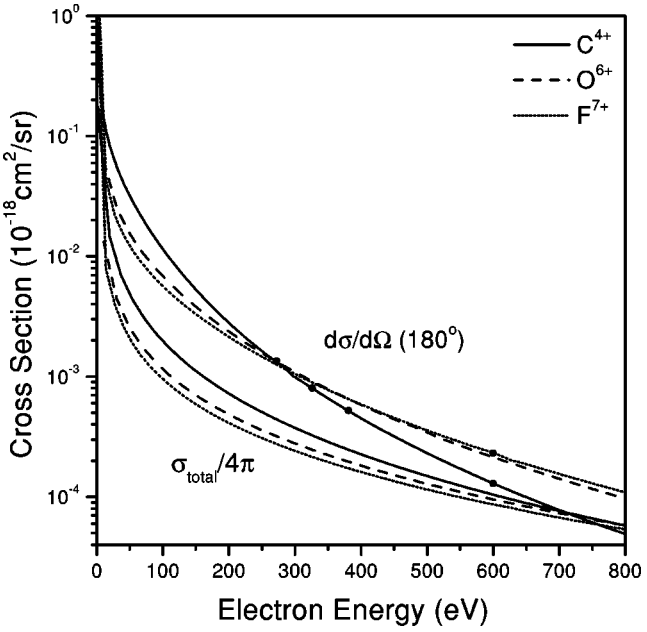

FIG. 3. Superelastic differential cross sections $d\sigma_{if}/d\Omega(180°)$ [from Eq. (3.2)] and $\sigma_{total}/4\pi$ [from Eq. (3.3)] for $1s2s\,^3S$ metastable C^{4+}, O^{6+}, and F^{7+} ions as a function of incident electron energy obtained from *R*-matrix calculations. The total cross sections (divided by 4π) are approximately inversely proportional to q^2, while the differential cross sections are larger and exhibit a different behavior that is clearly seen at the higher electron energies. The solid dots indicate the energies and ions investigated in this work.

rameter λ, giving rise to an anisotropy in the angular differential cross section that needs to be taken into account when compared with experiment. Then, the total cross section for superelastic scattering from an initial *S* state to a final *S* state is

$$\sigma_{total}=\int \frac{d\sigma_{if}}{d\Omega}d\Omega=\frac{\pi}{k_i^2}\sum_l (2l+1)|T_{ll}(i\rightarrow f)|^2. \tag{3.3}$$

It is emphasized that the energy dependences of σ_{total} and $d\sigma_{if}/d\Omega$ are not the same due to the anisotropy.

The differential and total superelastic cross sections [Eqs. (3.2) and (3.3), respectively] are inversely proportional to the electron-impact energy k_i^2. However, the differential cross section depends on the ionic charge of the He-like ion in a more complicated manner than the total cross section due to the presence of coherent sums of cross terms involving phase differences resulting from the various Coulomb phase shifts σ_l. Calculated differential cross sections and total cross sections divided by 4π are shown in Fig. 3 for the systems considered in this work.

The figure shows the calculated $d\sigma_{if}/d\Omega$ at 180° (in the projectile frame of reference) and $\sigma_{total}/4\pi$ for superelastic scattering from C^{4+}, O^{6+}, and F^{7+} ions as a function of the electron-impact energy. These cross sections demonstrate quantitatively the expected differences between isotropic cross sections and the actual cross sections that were measured in this work. It is seen that significant differences exist,

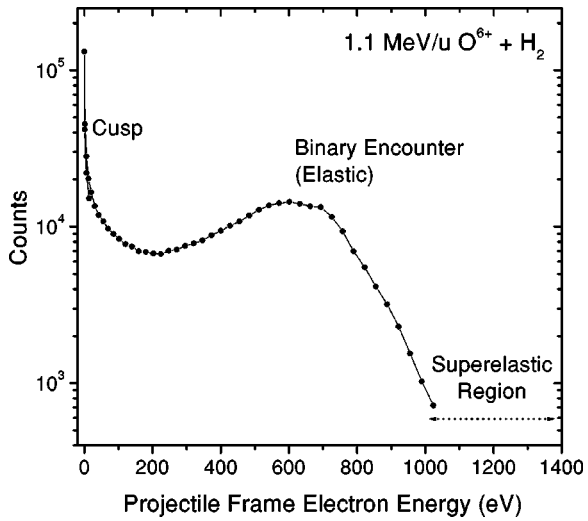

FIG. 4. Typical 0° electron-emission spectrum for 1.1-MeV/u $O^{6+}+H_2$ collisions in the projectile frame of reference. The cusp (electron capture or loss to the continuum) and binary-encounter (elastic-scattering) peaks are shown. The region for superelastic scattering is indicated in the figure.

both in magnitude and energy dependence, between assumed isotropic cross sections ($\lambda=0$ only) and the more rigorous anisotropic ones. In this regard, the total cross sections divided by 4π as a function of E/q^2, are proportional to q^{-4} [22], while the correct angle-dependent differential cross sections at 180° exhibit a different dependence on q as mentioned above [see Eq. (3.2)]. These differences between $d\sigma_{if}/d\Omega$ and $\sigma_{total}/4\pi$ will be important in the interpretation of the observed results discussed below.

IV. RESULTS AND DISCUSSION

A typical 0° spectrum for 1.1-MeV $O^{6+}+H_2$ collisions in the projectile frame of reference is shown in Fig. 4. The well-known cusp (free electrons traveling forward with the beam velocity) and binary-encounter (elastic-scattering) peaks are clearly seen in the spectrum. The cusp represents electrons that are captured to the continuum of the projectile or lost by the projectile to the continuum. The binary-encounter peak represents target electrons that are elastically scattered from the projectile ion. Thus, in the projectile frame of reference these electrons recoil with a velocity equal in magnitude and opposite in direction (at 180°) to the incident velocity.

Superelastically scattered electrons resulting from deexcitation of the $1s2s\,^3S$ metastable state are emitted on the high-energy side of the binary-encounter maximum, with an additional energy equal to the excitation energy of the metastable state above the ground state [see Eq. (1.1)]. Since the cross sections for superelastic scattering for the systems studied here are roughly four orders of magnitude smaller than those for elastic scattering [9], it is difficult to observe them directly from the spectrum. To observe superelastic-scattering events, the contribution from elastically scattered electrons (the binary-encounter peak) must be subtracted.

Differential cross sections for electrons emitted at 180°

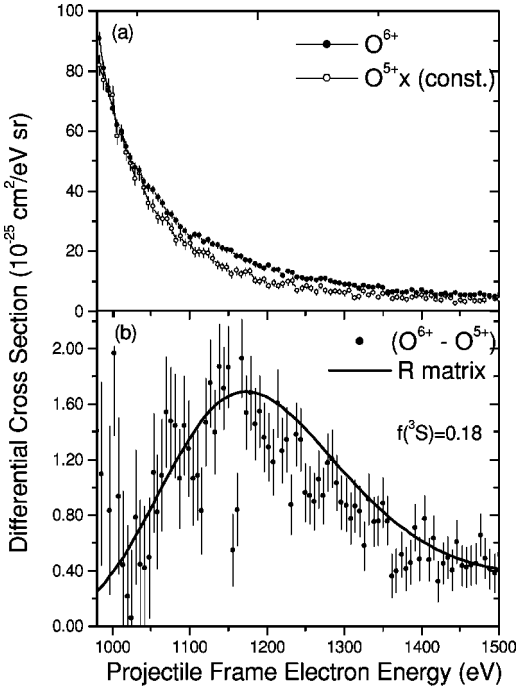

FIG. 5. Electron emission cross sections at 180° in the projectile frame of reference in the region of superelastic scattering for 1.1-MeV/u O^{6+} and $O^{5+}+H_2$ collisions. (a) Measured spectra for O^{6+} (solid circles) and O^{5+} (open circles) ions. The O^{6+} data contain a superelastic contribution in addition to the strongly dominating elastic part, while the O^{5+} spectrum is due only to elastic scattering. The O^{5+} data were normalized to the O^{6+} data in order to extract the superelastic scattering contribution (see text). (b) Superelastic scattering contribution (solid circles) resulting from subtraction of the O^{5+} data from the O^{6+} data in (a). The smooth curve is an R-matrix calculation for superelastic scattering obtained from the time-reversed process of inelastic electron scattering. The theory was multiplied by the factor 0.18 to account for the metastable $O^{6+}(1s2s\,^3S)$ fraction in the incident beam at this collision energy (see text).

(in the projectile frame of reference) with energies in the superelastic region were measured for O^{6+} ions as shown by the solid circles in Fig. 5(a). In order to extract the superelastic contribution to this spectrum, the dominating elastic-scattering contribution, i.e., that due to binary-encounter electrons, must be subtracted. Since Li-like ions do not have long-lived metastable states, no superelastic scattering is expected in collisions of these ions with electrons. The corresponding cross sections for incident Li-like O^{5+} ions, which can be used to subtract the elastic-scattering contribution, is shown by the open circles in Fig. 5(a). This latter spectrum was normalized to the O^{6+} data by choosing a multiplicative factor to cause the O^{5+} data to best match the O^{6+} data in the regions below and above the superelastic region. From the figure, a contribution to O^{6+} in excess of the O^{5+} elastic scattering is seen. This excess is attributed to superelastic scattering.

By subtracting the normalized O^{5+} spectrum from the O^{6+} spectrum, the result that remains is the superelastic-scattering cross section for O^{6+} ions as shown in Fig. 5(b), which exhibits a peak near 1170 eV. This value corresponds to the sum of the binary-encounter energy (elastic scattering) plus 570 eV, which is just the deexcitation energy of O^{6+} from the $1s2s\,^3S$ state to the $1s^2\,^1S$ state. The width of the peak is due to the Compton profile of the H_2-target electrons [23]. These same procedures were used to obtain the superelastic-scattering cross section for H_2-target electrons scattered from metastable 1.1-MeV/u $F^{7+}(1s2s\,^3S)$ in Ref. [9]. It is noted that superelastic scattering was also investigated in the present work for metastable 1.1-MeV/u F^{7+} ions to compare with the data of Ref. [9], and essentially identical results were obtained.

The smooth curve shown in Fig. 5(b) represents *R*-matrix calculations for superelastic scattering in the impulse approximation for the transition $O^{6+}[1s2s\,^3S]\rightarrow O^{6+}[1s^2\,^1S]$, taking into account the Compton profile of the target electrons and convoluting with the experimental energy resolution. In the calculations the He-like O^{6+} beam is assumed to have a 100% metastable fraction. Thus, the calculated superelastic cross section must be reduced by a factor to account for the metastable fraction present in the incident beam. By normalizing the theory to the data, shown by the curve in Fig. 5(b), a metastable fraction of 0.18 is obtained for the ^3S state, a value that is consistent with those obtained in Ref. [10] for $F^{7+}(1s2s\,^3S)$ beams of similar energy. The normalized theoretical curve shown in Fig. 5(b) agrees well with the observed maximum and width for superelastic scattering.

Superelastic scattering was also investigated for C^{4+} ions, for which several different collision energies were used. The resulting superelastic cross sections, after subtraction of the elastic-scattering background using the same procedures as for Fig. 5, are shown in Fig. 6 for 0.5-, 0.6-, and 0.7-MeV/u C^{4+} ions on H_2. These collision energies correspond to electron-impact energies of 272, 327, and 381 eV, respectively. Measurements were also made for 1.1-MeV/u C^{4+}, but no observable superelastic cross section was obtained. The energy scale used in the figure, $E_f - E_i = \Delta E$, corresponds to the energy gained by the electrons in the interaction. The peaks in these spectra are centered about an energy value of 298 eV, which is just the deexcitation energy of metastable C^{4+} from the $1s2s\,^3S$ state to the $1s^2\,^1S$ state. This shows that the outgoing electrons have been superelastically scattered in the interaction by gaining the energy lost by the metastable ion as it deexcites to the ground state.

R-matrix calculations for the different collision velocities are also shown in Fig. 6. In this case, the experimental data were normalized to the theory (for Fig. 5 the theory was normalized to the data), thereby giving the metastable fractions indicated in the figure. Thus, the curves shown in Fig. 6 represent the actual theoretical superelastic cross sections. It is again seen that the measured superelastic-scattering cross sections are in good agreement with the theory in both position and width, as was the case for the O^{6+} data shown in Fig. 5(b).

The strong energy dependence of the superelastic cross sections for C^{4+} ions seen in Fig. 6 can be explained by considering the calculated cross sections for this ion. Figure

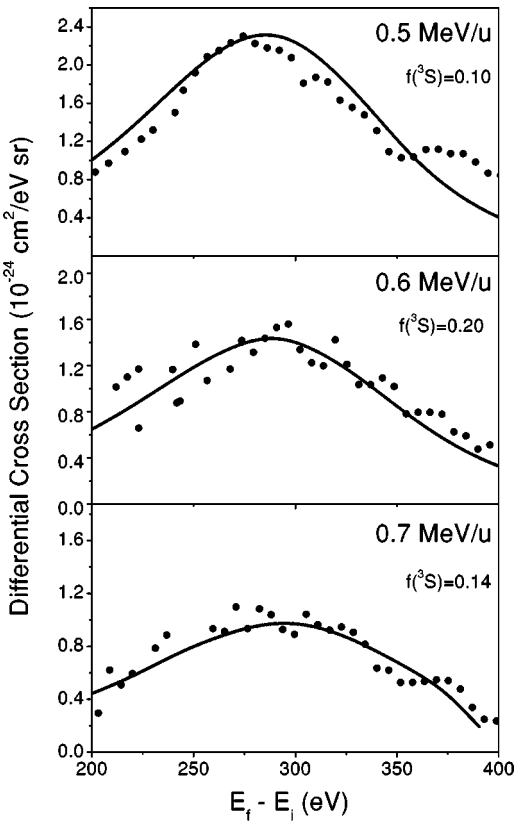

FIG. 6. Superelastic-differential-scattering cross sections at 180° for 0.5-, 0.6-, and 0.7-MeV/u $C^{4+}+H_2$ collisions. The dependence of the cross section on the collision energy is seen. The smooth curves are *R*-matrix calculations. The experimental data have been normalized to the theory, giving the metastable fractions indicated in the figure.

7 shows the calculated differential cross sections at 180° for superelastic scattering and its time-reversed equivalent (electron excitation) for $C^{4+}+H_2$ collisions, obtained from Eqs. (3.1) and (3.2). These cross sections are inversely proportional to the electron-impact energy. The superelastic cross section goes to infinity at zero impact energy, while the inelastic-scattering cross section, which corresponds to $1s^2\,{}^1S \rightarrow 1s2s\,{}^3S$ electron-impact excitation, has a threshold at an excitation energy $\sim$300 eV for this transition. The rapidly decreasing cross section explains the difficulty of obtaining a measurable result for 1.1-MeV/u (corresponding to $\sim$600 eV electron-impact energy) C^{4+} ions compared to the lower energies investigated for this ion.

The presence of the threshold excitation energy near 300 eV (see Fig. 7) is the reason that the measured metastable fraction for 0.5 MeV/u C^{4+}, which is just below the excitation threshold, is smaller than for the higher collision energies (see Fig. 6). This is because the probability for producing (in the post-stripping foil) the necessary metastable ions to observe superelastic scattering is smaller at this lower projectile energy. Despite the fact that 0.5 MeV/u lies below the threshold, metastable ions are still produced due to the rather broad width of the threshold for ion-atom collisions, a behavior that is well known for *K*-shell to *L*-shell excitation

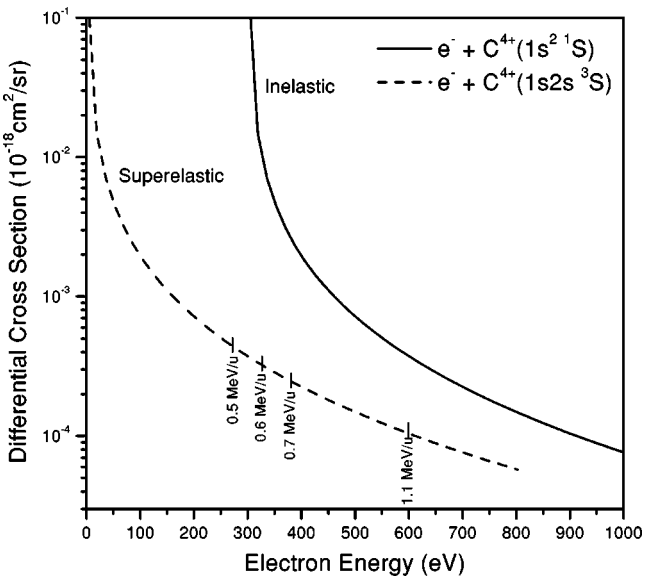

FIG. 7. Calculated differential cross sections for superelastic scattering, and the time-reversed process of electron-impact excitation, for e^-+C^{4+} collisions, as a function of incident-electron energy. The collision energies used in the experiment are indicated in the figure.

cross sections [24]. The smaller metastable fraction found for this energy is consistent with the findings of Ref. [10].

The behaviors of the differential cross sections shown in Fig. 3 also explain the difficulty of measuring superelastic scattering from C^{4+} ions at 1.1 MeV/u compared to O^{6+} and F^{7+} at the same collision energy. From this figure it is seen that $d\sigma_{if}/d\Omega$ (180°) for C^{4+} ions is more than two times smaller than for O^{6+} or F^{7+}. This result is to be contrasted with that expected if the cross section was isotropic, as shown by $\sigma_{total}/4\pi$ in Fig. 3, for which C^{4+} would have a larger cross section than O^{6+} and F^{7+}. In this latter regard, however, it is noted that the calculated anisotropic cross sections $d\sigma_{if}/d\Omega(180°)$ are larger than the isotropic $\sigma_{total}/4\pi$ over the energy range of the measurements conducted in this work. These observations demonstrate the importance of including angular dependence in the analysis and interpretation of measured superelastic cross sections.

V. CONCLUSIONS

Superelastic scattering of quasifree H_2-target electrons from C^{4+} and O^{6+} metastable ions has been investigated experimentally and theoretically. Measured cross sections for superelastic scattering show a strong dependence on the impact energy of the electrons and on the charge of the metastable ion. Calculated *R*-matrix cross sections for superelastic scattering were obtained from the time-reversed electron-impact-excitation cross sections using the principle of detailed balance. For the collisions with quasifree electrons considered here, the impulse approximation was utilized in conjunction with the Compton profile of the scattered electron. The calculated results show that the differential superelastic scattering cross section is approximately inversely proportional to the collision energy and exhibits a depen-

dence on the atomic number of the metastable ion, which differs significantly from that for the total scattering cross section. This anisotropy of the angular differential cross section was shown to be important in the interpretation of the measured cross sections for the different ions. By comparing experiment with theory it was possible to infer the metastable $1s2s\,^3S$ fractions of He-like ions present in the incident beam at each collision energy.

ACKNOWLEDGMENTS

This work was supported in part by the Chemical Sciences, Geosciences, and Biosciences Division, Office of Basic Energy Sciences, U.S. Department of Energy; T.W.G was supported in part by NASA, Space Astrophysics Research and Analysis Program, Grant No. NAG5-10448. We would like to thank D. C. Griffin for valuable discussions.

[1] N. Andersen, J.W. Gallagher, and I.V. Hertel, Phys. Rep. **165**, 1 (1988).
[2] Y. Li and P.W. Zetner, J. Phys. B **27**, L293 (1994).
[3] R.E. Scholten, G.F. Shen, and P.J.O. Teubner, J. Phys. B **26**, 987 (1993).
[4] I.D. Williams, J.B. Greenwood, and P. McGuinness, J. Phys. B **28**, L555 (1995).
[5] M. Jacka, M.D. Hoogerland, W. Lu, D. Milic, K.G.H. Baldwin, K. Bartschat, and S.J. Buckman, J. Phys. B **29**, L825 (1996).
[6] M.E. Bannister, X.Q. Guo, T.M. Kojima, and G.H. Dunn, Phys. Rev. Lett. **72**, 3336 (1994).
[7] K.A. Stockman, V. Karaganov, I. Bray, and P.J.O. Teubner, J. Phys. B **31**, L867 (1998).
[8] V. Karaganov, I. Bray, and P.J.O. Teubner, J. Phys. B **31**, L187 (1998).
[9] P.A. Závodosky, H. Aliabadi, C.P. Bhalla, P. Richard, G. Tóth, and J.A. Tanis, Phys. Rev. Lett. **87**, 332021 (2001).
[10] M. Terasawa, Tom J. Gray, S. Hagmann, J. Hall, J. Newcomb, P. Pepmiller, and Patrick Richard, Phys. Rev. A **27**, 2868 (1983).
[11] P. Eisenberger and P.M. Platzman, Phys. Rev. A **2**, 415 (1970).
[12] D. Brandt, Phys. Rev. A **27**, 1314 (1983).
[13] F. Bell, H. Böckl, M.Z. Wu, and H.-D. Betz, J. Phys. B **16**, 187 (1983).
[14] D.H. Lee, P. Richard, T.J.M. Zouros, J.M. Sanders, J.L. Shinpaugh, and H. Hidmi, Phys. Rev. A **41**, 4816 (1990).
[15] T.J.M. Zouros, in *Recombination of Atomic Ions*, edited by W.G. Graham, W. Fritsch, Y. Hahn, and J.A. Tanis (Plenum, New York, 1992), pp. 271–300.
[16] T.J.M. Zouros, K.L. Wong, S. Grabbe, H.I. Hidmi, P. Richard, E.C. Montenegro, J.M. Sanders, C. Liao, S. Hagmann, and C.P. Bhalla, Phys. Rev. A **53**, 2272 (1996).
[17] P. Hvelplund, A.D. González, P. Dahl, and C.P. Bhalla, Phys. Rev. A **49**, 2535 (1994).
[18] G. Tóth, S. Grabbe, P. Richard, and C.P. Bhalla, Phys. Rev. A **54**, R4613 (1996).
[19] P.A. Závodosky, G. Tóth, S.R. Grabbe, T.J.M. Zouros, P. Richard, C.P. Bhalla, and J.A. Tanis, J. Phys. B **32**, 4425 (1999).
[20] G.W. Drake, Phys. Rev. A **3**, 908 (1971).
[21] D.C. Griffin, M.S. Pindzola, and N.R. Badnell, Phys. Rev. A **47**, 2871 (1993).
[22] A. Burgess, D.G. Hummer, and J.A. Tully, Philos. Trans. R. Soc. London **266**, 225 (1970).
[23] J.S. Lee, J. Chem. Phys. **66**, 4906 (1977).
[24] M.R.C. McDowell and J.P. Coleman, *Introduction to the Theory of Ion-Atom Collisions* (North-Holland, Amsterdam, 1970), Chap. 7.